

Article

Mathematical Analysis of Transverse Wall-Shearing Motion via Cross Flow of Nanofluid

Faisal Z. Duraihem ¹, Arif Ullah Khan ², Salman Saleem ^{3,*} and Shawana ⁴¹ Department of Mathematics, College of Science, King Saud University, Riyadh 11451, Saudi Arabia² Department of Mathematics, Faculty of Natural Sciences, HITEC University, Taxila 47080, Pakistan³ Department of Mathematics, College of Science, King Khalid University, Abha 61413, Saudi Arabia⁴ Department of Mathematics, Gomal University, Dera Ismail Khan 29050, Pakistan

* Correspondence: saakhtar@kku.edu.sa

Abstract: The investigation of nanofluid's cross flow, which is caused by a nonlinear stretching sheet within the boundary layer, is presented. The proper mathematical detail is provided for three distinct cross flow instances with the streamwise flow. A uniform transverse stream located far above the stretched plate, in one instance, creates the cross flow. Two further situations deal with cross flows caused by surface transverse shearing motions. Weidman's work was used to find a similarity solution by making the necessary changes. It has been found that two parameters, namely nanoparticle volume fractions ϕ and a nonlinear stretching parameter β , have a significant impact on the flow of fluids in cross flow scenarios. Graphical representations of transverse and streamwise shear stresses and velocity profiles are provided. From this study, we found that nanoparticle volume fraction ϕ reduces the momentum boundary layer in both streamwise and cross flow scenarios while increasing the temperature of the fluid and, hence, increasing thermal boundary layer thickness. The same is observed for the nonlinear stretching parameter β .

Keywords: nanofluid; nonlinear stretching sheet; streamwise flow; cross flow; wall shear stress



Citation: Duraihem, F.Z.; Ullah Khan, A.; Saleem, S.; Shawana
Mathematical Analysis of Transverse Wall-Shearing Motion via Cross Flow of Nanofluid. *Lubricants* **2023**, *11*, 138. <https://doi.org/10.3390/lubricants11030138>

Received: 7 February 2023

Revised: 3 March 2023

Accepted: 12 March 2023

Published: 14 March 2023



Copyright: © 2023 by the authors. Licensee MDPI, Basel, Switzerland. This article is an open access article distributed under the terms and conditions of the Creative Commons Attribution (CC BY) license (<https://creativecommons.org/licenses/by/4.0/>).

1. Introduction

Boundary layer laminar flows have always remained significant in all eras for the development of fluid mechanics. Prandtl and Blasius were the first to study laminar flows over a flat plate with negligible viscosities [1,2]. Earlier, Prandtl [3] discussed the three-dimensional boundary layer flows with the assumptions of uniform pressure gradient. Later on, many researchers have contributed many developments in this field of three-dimensional boundary layer flows [4–7]. Takhar et al. [8] developed an unsteady three-dimensional boundary layer flow under the action of magnetohydrodynamic impulsive force over a stretching surface. Affes [9] considered a three-dimensional unsteady flow prompted by a vortex monofilament stirring a spherical tube externally. Ahmad et al. [10] studied the same kind of flows for micro polar fluids in stretching sheets.

The secondary flows, or cross flows, are significant phenomena in fluid mechanics due to their high demand in numerous industrial and engineering problems, such as aeronautics and spinning fluid problems. Weidman [11] found new cross-flow solutions inside a confined boundary layer. He addressed the problems of uniform laminar flow transverse to a wall, over a flat plate, transverse motion to a tangential plane, transverse uniform flow above and below a planar jet and transverse even streams above and underneath a planar laminar wake. Chu et al. [12] discussed the numerical results of cross flows in a stream way through a moving surface with magnetic force and viscous dissipative force. Dauenhauer [13] found a similarity solution of an incompressible laminar and steady fluid past a porous conduit with movable walls. Roşca et al. [14] studied the cross flow of a hybrid nano-fluid with heat transfer characteristics over a porous stretched surface and they discovered dual solutions in stability analysis, one of which (upper branch solution)

was physically reliable and the other (lower branch solution) was not. Weidman [15] found solutions within the boundary layer for laminar cross flows, in which he discussed the Blasius boundary layer streamwise flow for uniform plate motion and uniform tangential flow over a flat stretched surface. Rashidi et al. [16] developed a mathematical model for a streamwise fluid with transverse magnetic fields with heat transfer characteristics, and their main focus was to find the strength and direction of the magnetic field.

The similarity flows are the basic primary streamwise cross-flows that are mainly defined by nonlinear ODEs (ordinary differential equation) and secondary completely established flows that are of the type of cross flows defined by linear ODEs having variable coefficients and basic primary flow solution. Bhattacharyya and Pop [17] studied the properties of heat transfer by finding out the dual solution of boundary layer cross flows. Zhong et al. [18] discussed approaching boundary layers with the involvement of different coolants and concluded that the circulation of photo-moving preservation consequences fluctuated close to the principal edge. Yufeng et al. [19] numerically investigated the solution of cross flow conversion in 3-D hypersonic boundary layer flows.

Many engineering applications have flows over stretching surfaces, such as chemical industries and metallurgy departments in industries which require the cooling of filament strips by a continuous process. Crane [20] was the first to study the influence of fluid flow over a stretching surface. It opened the gates to a new way of research for scientists to explore the flow over stretching surfaces and a good amount of this research work is available in the literature [21–30]. Since then, a no slip boundary condition occurs for a small flow system with low pressure of fluid so that it can be neglected but this case is not appropriate for all situations. In this case, assumptions of Navier [31] are employed, i.e., the tangential component of fluid's velocity at the boundary is directly proportional to tangential stresses. Martin et al. [32] discussed this slip boundary condition for Blasius' problem. Rao and Rajagopal [33] investigated linear viscous fluid's flow past an extending surface with velocity slip-boundary conditions in a channel. Ellahi [34] explored the slip boundary conditions for non-Newtonian fluids in a channel. Hayat et al. [35] explored the dependence of slip velocity on shear stresses for nonlinear flows. There are numerous studies of fluid flows over stretching surfaces [36–39], but all those mentioned in the literature are about linear stretching surfaces.

It is important to note that nonlinear stretching is applicable in many manufacturing industries in the current research era and should not be limited to just linear stretching. Some examples include the extrusion of polymer sheets, hot rolling, bundle wrapping, extrusion of sheet material, wire rolling and glass fiber. Nonlinear stretching has recently captured the interest of numerous scholars. For the very first time, the importance of nonlinear stretching was brought to notice by Gupta with Gupta [40], in which they discussed heat and mass transfer analysis over a nonlinear stretched sheet with suction and blowing. Vajravelu [41] carried out his research for viscous fluid over a nonlinear stretching surface, and his work was extended by Cortell [42] for heat transfer analysis by considering a nonlinear stretching surface with fixed surface temperature and with prescribed surface temperature. Das [43] explored nanofluid flow over a nonlinear stretched permeable surface in the presence of a boundary at partial slip. Seth and Mishra [44] considered the Navier slip boundary condition at a nonlinear stretched sheet for magnetic nanofluid flow. Mukhopadhyay [45] explored the fluid's flow within the boundary layer past a nonlinear absorbent extending surface with partial slip condition.

The most frequently discussed issue now is nanofluids with remarkable heat transit properties, which have amazing heat-transfer characteristics in comparison to typical heat-transit fluids. In universal heat-transfer fluids, such as ethylene glycol, water, oil, etc., nanoparticles less than 100 nm in size can be found in nanofluids. Nanofluids provide a unique advantage over conventional heat-transfer fluids. A very small amount of nanoparticles that are fully suspended and regularly dispersed in the base fluids cause sensational development in the thermal effects of the parent fluids. One-step and two-step procedures are used to create stable and highly conducted nanofluids. However, while producing

nanoparticles, both methods produce clusters of nanoparticles. This is the key problem in industrial science, particularly with nano powder. Choi [46] came up with the term “nanofluid”, which describes how the addition of nanoparticles significantly improves the thermal properties of basic fluids. Many researchers have implications for adding nanoparticles to the drain flow because of this considerable research. An experimental analysis of Choi’s results was conducted by Kang et al. in [47]. The existence of all these exciting applications has propelled scholars to explore new directions in the study of magnetic characteristics and nanofluid flow [48–56].

All the cited studies employ numerical techniques or a perturbation approach to arrive at the nanofluid solution over a nonlinear stretching sheet. There are only a relatively small number of research situations in the literature where the exact solution for the nanofluid over a nonlinear stretching sheet has been found. These exact analytical results for a nonlinear stretching sheet are extremely uncommon.

The main motivation is to fill the gap and connect the above-cited literature with the new developments. Therefore, we consider Cu-water nanofluid towards a nonlinear stretching sheet and find analytic solutions for some special cases of stretching parameters. Here, streamwise flows are under consideration along with three different categories, namely:

- Cross flow in the presence of a uniform free stream;
- Cross flow in the presence of a transverse moving surface;
- Cross flow in the presence of a transverse surface shearing movement.

The streamwise flow and all the cases of cross flow depend upon the two parameters, namely nanoparticle volume fractions ϕ and nonlinear stretching parameter β . Streamwise and transverse shear stresses and the fluid’s behavior towards pertinent parameters are presented graphically.

2. Theoretical Development

We took into account the incompressible Cu-water nanofluid flowing over a rigid horizontal nonlinear stretching plate. As illustrated in Figure 1, the plate has been set at $y = 0$ and the coordinate system (x, y, z) with corresponding velocity (u, v, w) has been assumed. The streamwise flow is produced along the x -direction, the cross flow is directed along the z -direction and y is the plate normal coordinate. We assume that all flows are fully developed in the spanwise direction. Therefore, we look for solutions with velocity fields independent of the spanwise coordinate z . Thus, the law of conservation of mass is as follows [57]

$$\frac{\partial u}{\partial x} + \frac{\partial v}{\partial y} = 0 \quad (1)$$

and modified properties boundary layer equations are [57]

$$u \frac{\partial u}{\partial x} + v \frac{\partial u}{\partial y} + \frac{1}{\rho} \frac{\partial p}{\partial x} = \nu_{nf} \left(\frac{\partial^2 u}{\partial x^2} + \frac{\partial^2 u}{\partial y^2} \right) \quad (2)$$

$$u \frac{\partial v}{\partial x} + v \frac{\partial v}{\partial y} + \frac{1}{\rho} \frac{\partial p}{\partial y} = \nu_{nf} \left(\frac{\partial^2 v}{\partial x^2} + \frac{\partial^2 v}{\partial y^2} \right) \quad (3)$$

$$u \frac{\partial w}{\partial x} + v \frac{\partial w}{\partial y} + \frac{1}{\rho} \frac{\partial p}{\partial z} = \nu_{nf} \left(\frac{\partial^2 w}{\partial x^2} + \frac{\partial^2 w}{\partial y^2} \right) \quad (4)$$

$$u \frac{\partial T}{\partial x} + v \frac{\partial T}{\partial y} = \alpha_{nf} \left(\frac{\partial^2 T}{\partial x^2} + \frac{\partial^2 T}{\partial y^2} \right) \quad (5)$$

where $\nu_{nf} = \frac{\mu_{nf}}{\rho_{nf}}$ is its kinematic viscosity; ρ_{nf} is nanofluid density; μ_{nf} is the dynamic viscosity of nanofluid; $\alpha_{nf} = \frac{k_{nf}}{(\rho C_p)_{nf}}$ represents effective thermal diffusivity; k_{nf} is effective thermal conductivity and $(\rho C_p)_{nf}$ represent heat capacity of nanofluid and are defined as

$$\rho_{nf} = (1 - \phi)\rho_f + \phi\rho_s$$

$$\mu_{nf} = \frac{\mu_f}{(1 - \phi)^{2.5}}$$

$$k_{nf} = k_f \frac{(k_s + 2k_f) - 2\phi(k_f - k_s)}{(k_s + 2k_f) + \phi(k_f - k_s)}$$

$$(\rho C_p)_{nf} = (1 - \phi)(\rho C_p)_f + \phi(\rho C_p)_s$$

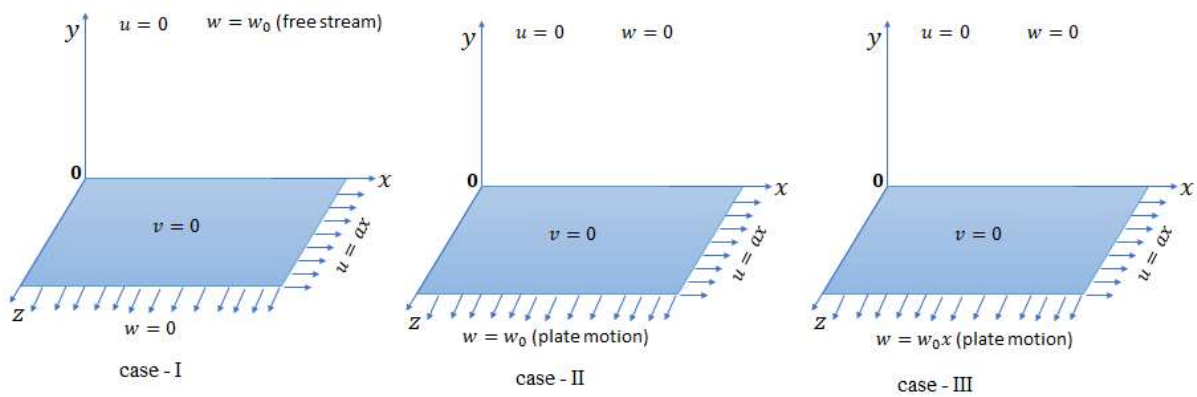


Figure 1. Geometry of the problem.

Here ϕ is the nanofluid volume fraction ρ_f is the density of base fluid, ρ_s is the density of the nanoparticle, μ_f is the dynamic viscosity of base fluid, k_f is the thermal conductivity of base fluid, k_s is the thermal conductivity of nanoparticle, $(\rho C_p)_f$ is the heat capacity of base fluid and $(\rho C_p)_s$ is the heat capacity of nanoparticle. The thermophysical properties of the base fluid and nanoparticles are defined in Table 1. Since the flow is measured to have no outside pressure gradient, Equation (4) is ignored. Thus, by applying boundary layer approximation [57], Navier–Stokes’ equation of streamwise and cross flow and heat equation is reduced to

$$u \frac{\partial u}{\partial x} + v \frac{\partial u}{\partial y} = \nu_{nf} \frac{\partial^2 u}{\partial y^2} \tag{6}$$

$$u \frac{\partial w}{\partial x} + v \frac{\partial w}{\partial y} = \nu_{nf} \frac{\partial^2 w}{\partial y^2} \tag{7}$$

$$u \frac{\partial T}{\partial x} + v \frac{\partial T}{\partial y} = \alpha_{nf} \frac{\partial^2 T}{\partial y^2} \tag{8}$$

2.1. Nonlinear Stretching Surfaces

We employ the similarity solution suggested by [57] to examine the streamwise flow caused by the movement of a nonlinear stretching sheet with velocity $u = ax^m$

$$u(x, y) = ax^m f'(\eta), \quad \eta(x, y) = \sqrt{\frac{a(m+1)}{2\nu_f}} x^{(m-1)/2} y \tag{9}$$

$$v(x, y) = -\sqrt{\frac{av_f(m+1)}{2}} x^{(m-1)/2} \left[f(\eta) + \left(\frac{m-1}{m+1}\right) \eta f'(\eta) \right] \tag{10}$$

Inserting Equations (7) and (8) in Equation (5), we deduced that

$$\frac{\nu_{nf}}{\nu_f} f''' + f f'' - \beta f'^2 = 0, \quad f(0) = 0, \quad f'(0) = 1, \quad f'(\infty) = 0 \quad (11)$$

where $\beta = 2m/(m+1)$. For $\phi = 0$, one shows that the solution for Equation (11) is possible when $-1.9999 \leq \beta \leq 202$. However later on, Bank [58] proved that for $-2 < \beta \leq 2$ the plate causes stretching motion, whereas for $2 < \beta < \infty$ the plate causes shrinking. In the present study, we assume only stretching motion.

Table 1. Thermophysical properties of fluid and nanoparticles [59].

Thermophysical Properties	Fluid Phase (Water)	Copper (Cu)
C_p (J/kgK)	4179	385
ρ (kg/m ³)	997.1	8933
k (W/mK)	0.613	400

Longitudinal shear stress in dimensional form becomes

$$\begin{aligned} \tau_x &= \left(\frac{\mu_{nf}}{\mu_f} \right) \mu_f \frac{\partial u}{\partial y} \Big|_{y=0} \\ &= \left(\frac{\mu_{nf}}{\mu_f} \right) \mu_f a \sqrt{\frac{a(m+1)}{2\nu_f}} x^{(3m-1)/2} f''(0) \end{aligned} \quad (12)$$

Equation (12) is a high Reynold's number equation and the solution of this equation represents the nature of streamwise flow.

2.2. Uniform Free Stream and Crosswise Plate Motion

In this section, we discuss cross flow induced by (i) uniform freestream and (ii) transverse plate motion. In both cases, the similarity variable is defined as [57]

$$w(x, y) = \begin{cases} w_0 g_1(\eta), & \text{for free stream} \\ w_0 g_2(\eta), & \text{for plate motion} \end{cases} \quad (13)$$

Here w_0 is constant, which represents the strength of crossflow in both cases g_1 and g_2 . Making use of Equations (9), (10) and (13), we deduce from Equation (7) as

$$\text{Free stream case} \quad \frac{\nu_{nf}}{\nu_f} g''_1 + f g'_1 = 0, \quad g_1(0) = 0, \quad g_1(\infty) = 1, \quad (14)$$

$$\text{Plate motion case} \quad \frac{\nu_{nf}}{\nu_f} g''_2 + f g'_2 = 0, \quad g_2(0) = 1, \quad g_2(\infty) = 0. \quad (15)$$

In both cases, transverse shear stress at the wall is given below

$$\begin{aligned} \tau_z &= \left(\frac{\mu_{nf}}{\mu_f} \right) \mu_f \frac{\partial w}{\partial y} \Big|_{y=0} \\ &= \left(\frac{\mu_{nf}}{\mu_f} \right) \mu_f w_0 \sqrt{\frac{a(m+1)}{2\nu_f}} x^{(m-1)/2} g'_1(0) \end{aligned} \quad (16)$$

2.3. Exceptional Cases for $g_1(\eta)$

Exceptional cases of $g_1(\eta)$ flow are considered for various values of $\beta = (1, 0, -1)$. When $\alpha = 1$, it is observed that streamwise flows instigated by [54] hold an exact solution

for $f(\eta) = \sqrt{\frac{\nu_{nf}}{\nu_f}} \left(1 - e^{-\frac{\eta}{\sqrt{\frac{\nu_{nf}}{\nu_f}}}} \right)$. Using this solution in Equation (14), becomes

$$\frac{\nu_{nf}}{\nu_f} g''_1 + \sqrt{\frac{\nu_{nf}}{\nu_f}} \left(1 - e^{-\frac{\eta}{\sqrt{\frac{\nu_{nf}}{\nu_f}}}} \right) g'_1 = 0, \quad g_1(0) = 0, \quad g_1(\infty) = 1 \tag{17}$$

which has the solution

$$g_1(\eta) = \frac{e}{e-1} \left[e^{-e^{\frac{-\eta}{\sqrt{\frac{\nu_{nf}}{\nu_f}}}}} - \frac{1}{e} \right] \tag{18}$$

From Equation (18), we obtain the transverse shear stress parameter $g'_1(0)$ as

$$g'_1(0) = \frac{1}{(e-1)\sqrt{\frac{\nu_{nf}}{\nu_f}}} = 0.581977 \frac{1}{\sqrt{\frac{\nu_{nf}}{\nu_f}}} \tag{19}$$

In addition, for $\beta = 0$, Equation (11) will be reduced as $\frac{\nu_{nf}}{\nu_f} f''' + ff'' = 0$ and, after comparing it with Equation (14) and their boundary conditions, we obtain

$$g_1(\eta) = 1 - f'(\eta) \tag{20}$$

We can show the above relation by computing numerical results.

Furthermore, for $\beta = -1$ we obtained the exact solution of Equation (11) as

$$f(\eta) = \sqrt{2} \left(\sqrt{\frac{\nu_{nf}}{\nu_f}} \right) \tanh \left(\frac{\eta}{\sqrt{2} \left(\sqrt{\frac{\nu_{nf}}{\nu_f}} \right)} \right) \tag{21}$$

On substituting Equation (21) into Equation (14) and solving gives

$$g_1(\eta) = \tanh \left(\frac{\eta}{\sqrt{2} \left(\sqrt{\frac{\nu_{nf}}{\nu_f}} \right)} \right) \tag{22}$$

so cross flow shear stress becomes

$$g'_1(0) = \frac{1}{\sqrt{2} \left(\sqrt{\frac{\nu_{nf}}{\nu_f}} \right)} \tag{23}$$

2.4. Association between Two Solutions

An examination of a governed system with BVP (Equations (14) and (15)) shows the connection of the solution

$$g_2(\eta) = 1 - g_1(\eta), \quad g'_2(0) = -g'_1(0) \tag{24}$$

Firstly, the boundary values for $g_1(\eta)$ are considered from which results are construed for $g_2(\eta)$.

To ascertain the above symmetry in Equation (24), we obtained the numerical results of the coupled system (Equations (11), (14), and (15) for the parametric ranges $-2 < \beta \leq 2$

and $0 < \phi \leq 0.2$. The results of longitudinal shear stress constraint $f''(0)$, transverse shear stress constraints $g'_1(0)$ and $g'_2(0)$, streamwise velocity $f(\eta)$ and cross flow velocity profiles $g'_1(\eta)$ and $g'_2(\eta)$ are displayed in figures as a function of β and ϕ .

3. Transverse Wall Shearing Motion

Transverse shearing motion is responsible for producing cross flow with streamwise flow past a stretched wall. This transverse motion is measured as [54]

$$w(x, 0) = w_0x^\sigma \tag{25}$$

where w_0 is pseudo velocity with different components for each power of σ . Similarity solutions are taken as

$$w(x, y) = w_0x^\sigma g(\eta) \tag{26}$$

Making use of similarity variables (9,10,26), Equation (7) reduces to

$$\frac{v_{nf}}{v_f} g'' + fg' - \frac{2\sigma}{m+1} f'g = 0, \quad g(0) = 1, \quad g(\infty) = 0 \tag{27}$$

Equation (27) shows it is true for any value of σ . However, this set of equations depends on three parameters, namely ϕ , β and $\sigma(m)$. Yet, two-parameter families of solutions depend on both ϕ β for two selections.

Details are deliberated below as $\sigma = \begin{cases} \frac{(m+1)}{2} \\ nm, \text{ for } n \text{ to be an integer} \end{cases}$.

3.1. For Case $\sigma = (m + 1)/2$

Here for this case, the boundary value problem in Equation (27) reduces to

$$\frac{v_{nf}}{v_f} g'' + fg' - f'g = 0, \quad g(0) = 1, \quad g(\infty) = 0 \tag{28}$$

We see that now Equation (28) depends on two parameters, namely, β and ϕ . To solve this equation numerically, we see the special case for g solution when $\beta = 1$ whereby f

solution $f = \sqrt{\frac{v_{nf}}{v_f}} \left(1 - e^{-\frac{\eta}{\sqrt{\frac{v_{nf}}{v_f}}}} \right)$ prevails. Inserting this into Equation (28), we obtained the analytic solution as follows

$$g(\eta) = e^{-\frac{\eta}{\sqrt{\frac{v_{nf}}{v_f}}}}, \quad g'(0) = -\frac{1}{\sqrt{\frac{v_{nf}}{v_f}}} \tag{29}$$

The wall-shear stress parameter for transverse wall-shearing motion is

$$\begin{aligned} \tau_z \Big|_{y=0} &= \left(\frac{\mu_{nf}}{\mu_f} \right) \mu_f \frac{\partial w}{\partial y} \Big|_{y=0} \\ &= \left(\frac{\mu_{nf}}{\mu_f} \right) \mu_f w_0 \sqrt{\frac{a(m+1)}{2v_f}} x^{(2\sigma+m-1)/2} g'_1(0) \end{aligned} \tag{30}$$

Computational results for shear stress at wall $g'(0)$ in the segment $-2 < \beta \leq 2$ and $0 \leq \phi \leq 0.2$ are exposed in the figures.

3.2. For Case $\sigma = nm$

Here it is assumed that n is an integer. Thus, Equation (27) reduces to

$$\left(\frac{v_{nf}}{v_f}\right)g'' + fg' - n\alpha f'g = 0, \quad g(0) = 1, \quad g(\infty) = 0 \quad (31)$$

Now, the parameters α and ϕ explicitly appear in both primary and secondary equations, that is f and g . To solve Equation (31) numerically, first we must discuss some special cases for n . In the first case, by substituting $n = 1$ and $g(\eta) = f'(\eta)$ in Equation (31), we obtained the same boundary value problem as in Equation (11). Consequently, the wall shear stress constraint is related by $g'(0) = f''(0)$ and crossflow velocity $g(\eta)$ remains similar to streamwise $f'(\eta)$ for all values of α and ϕ .

For $n = 2$, Equation (31) becomes

$$\frac{v_{nf}}{v_f}g'' + fg' - 2\alpha f'g = 0, \quad g(0) = 1, \quad g(\infty) = 0 \quad (32)$$

Some solutions and special relations are available for Equation (32). First, with $\beta = -1$ corresponding to $f(\eta)$ solution in Equation (21), the exact solution for Equation (32) is as follows

$$g(\eta) = \operatorname{sech}^2\left(\frac{\eta}{\sqrt{2}\left(\sqrt{\frac{v_{nf}}{v_f}}\right)}\right), \quad g'(0) = 0 \quad (33)$$

For $\beta = 0$, this implies $g(\eta) = 1 - f'(\eta)$.

For $\beta = 1$, $f(\eta) = \sqrt{\frac{v_{nf}}{v_f}} \left(1 - e^{-\frac{\eta}{\sqrt{\frac{v_{nf}}{v_f}}}}\right)$ the exact solution for cross flows becomes

$$g(\eta) = \frac{1}{3} \left(2e^{-\frac{\eta}{\sqrt{\frac{v_{nf}}{v_f}}}} + e^{-\frac{2\eta}{\sqrt{\frac{v_{nf}}{v_f}}}}\right), \quad g'(0) = -\frac{4}{3} \frac{1}{\sqrt{\frac{v_{nf}}{v_f}}} \quad (34)$$

For $\sigma = 2m$, the cross flow wall shear stress at the wall becomes

$$\begin{aligned} \tau_z \Big|_{y=0} &= \left(\frac{\mu_{nf}}{\mu_f}\right) \mu_f \frac{\partial w}{\partial y} \Big|_{y=0} \\ &= \left(\frac{\mu_{nf}}{\mu_f}\right) \mu_f w_0 \sqrt{\frac{a(m+1)}{2v_f}} x^{(5m-1)/2} g'_1(0) \end{aligned} \quad (35)$$

Computational values for shear stress constraints for a given choice of $-2 < \beta \leq 2$ and $0 \leq \phi \leq 0.2$ are exposed.

4. Heat Transfer

In the heat transfer phenomenon, we discuss two cases. Case-I is for a constant heated surface, $T_w = \text{constant}$ with ambient temperature $T_\infty < T_w$, while case-II is for a variable heated surface, $T_w = Dx + T_\infty$ with ambient temperature T_∞ . D is constant, having a dimension of temperature over length. If the constant D is negative (positive), then the surface is colder (hotter) than the surrounding at $x > 0$. The similarity solution for both cases is assumed as

$$\theta(\eta) = \frac{T - T_\infty}{T_w - T_\infty} \quad (36)$$

Using the above similarity variables, Equation (8) for both cases, with their boundary constraints, becomes

$$\text{Case - I} \quad \frac{1}{Pr} \frac{\alpha_{nf}}{\alpha_f} \theta'' - f\theta' = 0, \theta(0) = 1, \theta(\infty) = 0 \quad (37)$$

$$\text{Case - II} \quad \frac{1}{Pr} \frac{\alpha_{nf}}{\alpha_f} \theta'' + f\theta' - f'\theta = 0, \theta(0) = 1, \theta(\infty) = 0 \quad (38)$$

The physical quantity of interest related to the temperature profile is the heat flux at the surface, which is defined as

$$q_w = -k_{nf} \left. \frac{\partial T}{\partial y} \right|_{y=0} \quad (39)$$

$$q_w = -\frac{k_{nf}}{k_f} k_f (T_w - T_\infty) \sqrt{\frac{a(m+1)}{2\nu_f}} x^{(m-1)/2} \theta'(0)$$

We obtained the numerical results for the flow field over the large parameter range $-2 < \beta \leq 2$ and $0 < \phi \leq 0.2$ while taking $Pr = 6.2$ as a constant throughout the computation. The results of longitudinal shear stress constraint $f''(0)$, transverse shear stress constraint $g'_1(0)$, $g'_2(0)$ and $g'(0)$, wall heat flux $-\theta'(0)$, streamwise velocity $f(\eta)$ and cross flow velocity profiles $g_1(\eta)$, $g_2(\eta)$, $g(\eta)$ and temperature profile $\theta(\eta)$ are displayed in figures as a function of β and ϕ .

5. Result and Discussions

Here, the cross-flow phenomenon occurs due to the uniform transverse free stream and the second type of cross flow is produced when the stretching sheet has movement with uniform velocity. On the other hand, the movement of the transverse shearing surface is responsible for the third kind of cross flow.

We obtain the three-parameter scheme of equations that depends on ϕ , β and $\sigma(m)$. However, the two-parameter families of solutions are dependent on both ϕ and β for existing selections $\sigma = \begin{cases} \frac{(m+1)}{2} \\ nm, \text{ for } n \text{ to be an integer} \end{cases}$. We obtained some closed-form solution against the selected values of $\beta = (-1, 0, 1)$ for all types of cross flow and streamwise flow while, for a large range of $-2 < \beta \leq 2$, we obtained numerical results by using the BVP4c routine in MATLAB.

While comparing the present results, it is found that Weidman's solutions [34] are retained in the absence of ϕ . Figure 2 is plotted to show the behavior of streamwise flow $f'(\eta)$ against nonlinear stretching parameter β and nanoparticle volume fraction ϕ . It is observed that both parameters control the streamwise boundary layer thickness and force to reduce it. Figure 3 represents the cross flow velocity components $g_1(\eta)$ and $g_2(\eta)$ for values of the nonlinear stretching parameter β and nanoparticle volume fraction ϕ . It is clearly seen that by changing the value of β from zero to negative, the cross flow velocity $g_1(\eta)$ increases and $g_2(\eta)$ decreases while the boundary layer thickness of both components decreases. On the other hand, the phenomenon is just the opposite for positive values of β . Furthermore, ϕ enhances the magnitude of the velocity g_1 and shrinks the velocity g_2 . Figure 4 represents cross-stream similarity sketches $g(\eta)$ for transverse plate shearing motion with $\sigma = 2m$. It is observed that both parameters play a vital role in shrinking the cross flow boundary layer thickness. Moreover, it is depicted that streamwise wall-shear stress constraints $f''(0)$ is a divergent function of β when $\beta \rightarrow -2$ as shown in Figure 5. Furthermore, we deduced that $f''(0) = 0$ at $\alpha = -1$ for all values of β , which is the value of the exact solution in Equation (2). In addition, from Figure 5, as $f''(0, \beta, \phi)$ as a function of ϕ changes its behavior at $\beta = -1$, $f''(0, \beta, -1 < \alpha \leq 2)$ is a decreasing function of ϕ , whereas $f''(0, \beta, -2 < \alpha < -1)$ is an increasing function of ϕ . Similarly, the behavior is the same for the streamwise wall-shear stress parameter $f''(0)$. It is pertinent from Figure 6 that cross flow shear stress parameters $g'_1(0)$ and $g'_2(0)$ show blow-up behavior at $\beta = -2$.

In addition, it is included that $g'_1(0)$ and $g'_2(0)$ are mirror images of one another and show the symmetry relation in Equation (23) which guarantees the accuracy of the obtained numerical results. Figure 7 presents the transverse shear stress parameter $g'(0)$ for the case $\sigma = 2m$. We see that $g'(0)$ shows singularities for the case $\sigma = 2m$. The singularity separates the lower and upper branches at β_c , where β_c is weakly dependent upon ϕ . It is observed that thermal boundary layer thickness enhances for both the nonlinear stretching parameter β and nanoparticle volume fraction ϕ , respectively (see Figure 8). It is noticed in Figure 9 that the heat flux $-\theta(0)$ is a weak function of nonlinear stretching parameter β while the aptitude is contrasted for nanoparticle volume fraction ϕ . It is obtained that heat flux has a higher value in case-II compared to case-I.

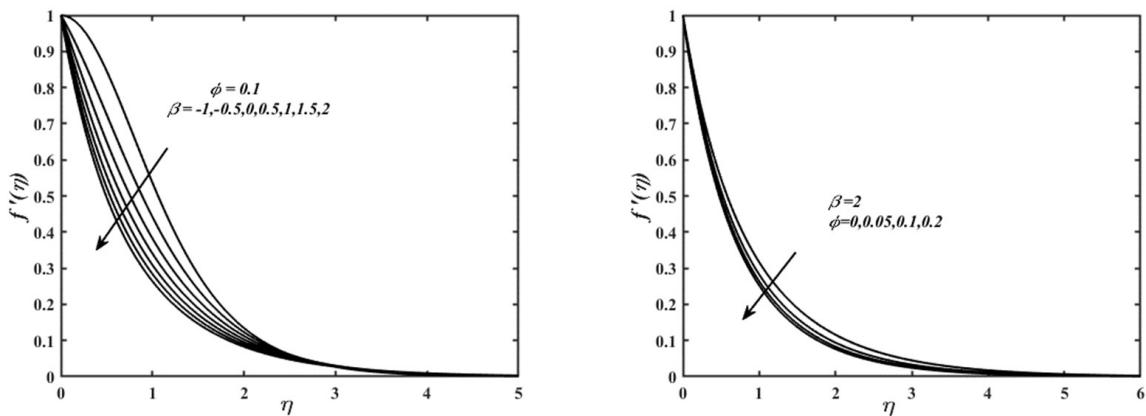


Figure 2. Streamwise flow velocity profiles $f'(\eta)$ for different values of β and ϕ .

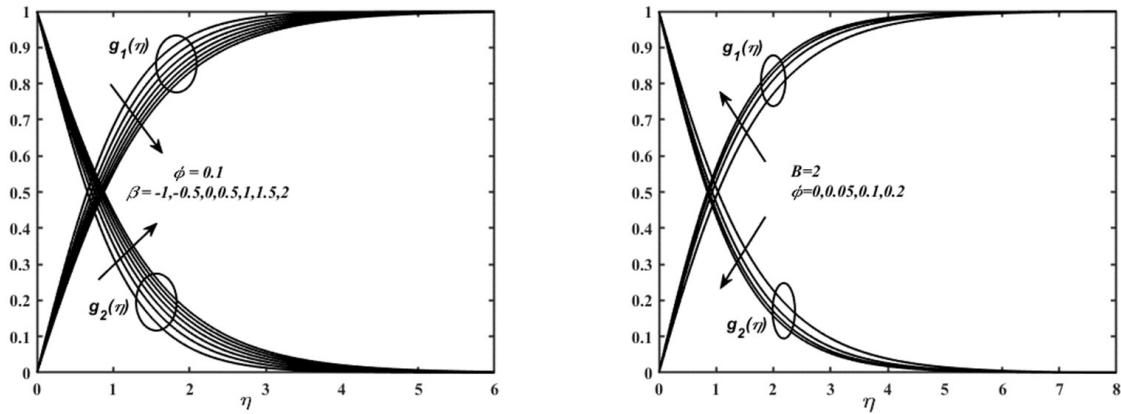


Figure 3. Cross flow velocity profiles $g_1(\eta)$ and $g_2(\eta)$ for different values of β and ϕ .

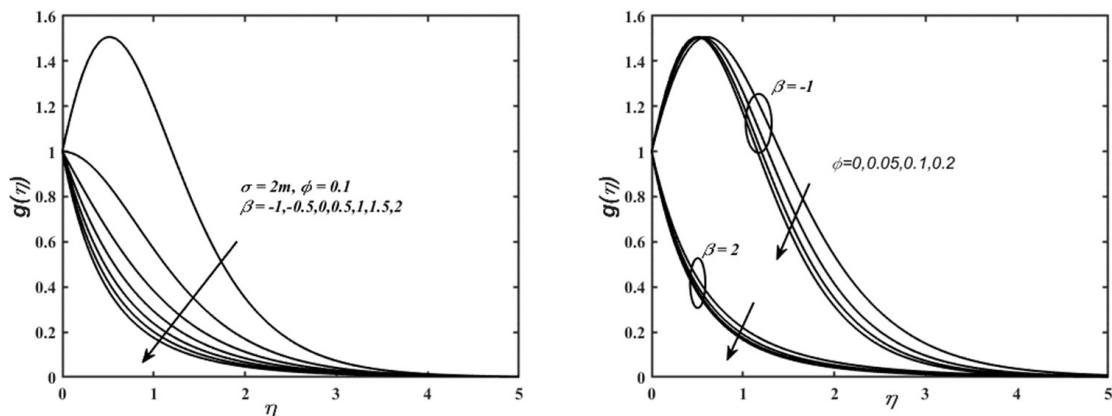


Figure 4. Cross stream similarity sketches $g(\eta)$ for transverse wall-shearing motion with $\sigma = 2m$.

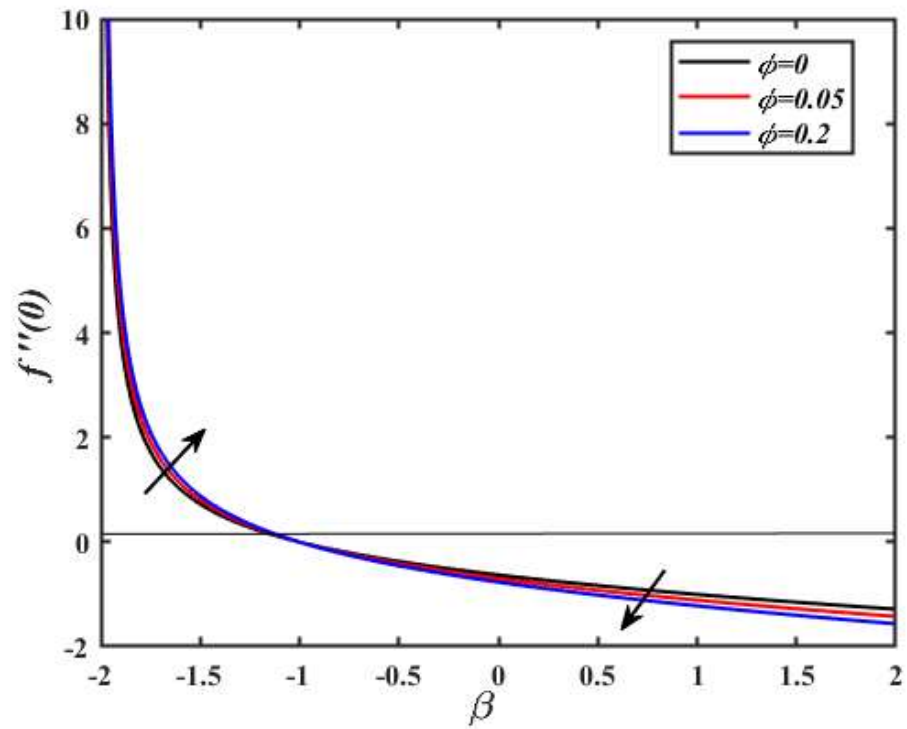


Figure 5. Streamwise wall-shear stress parameter $f''(0)$ as a function of β for various $\phi = \{0, 0.05, 0.2\}$. The arrow shows course of cumulative ϕ .

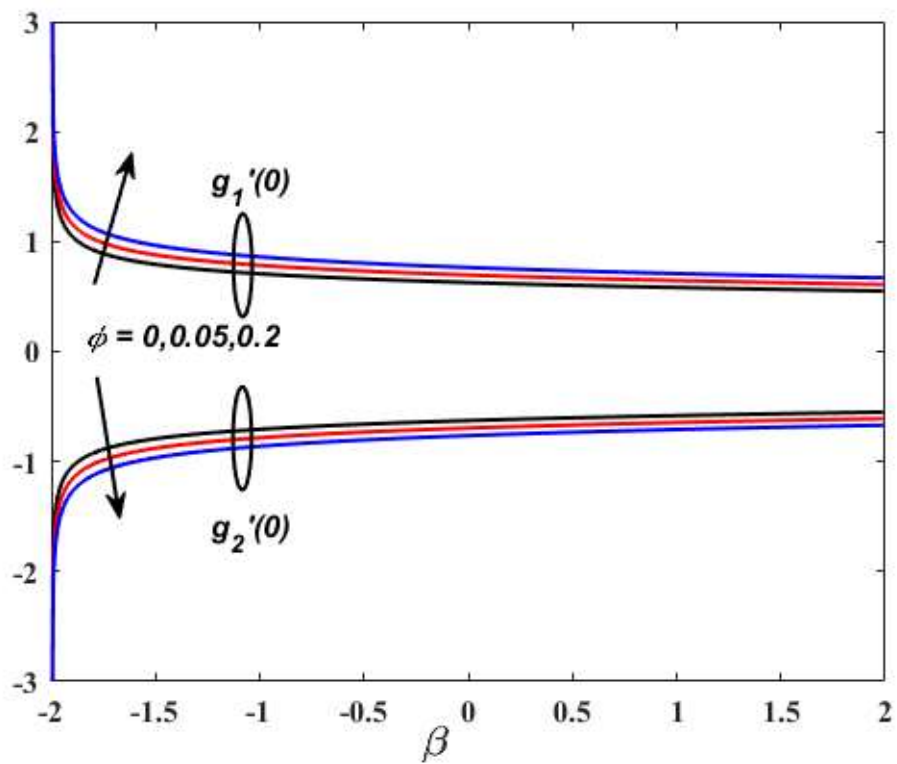


Figure 6. Cross flow wall-shear stress parameters $g'_1(\eta)$ and $g'_2(\eta)$ as a function of β for various $\phi = \{0, 0.05, 0.2\}$. The arrow shows course of cumulative ϕ .

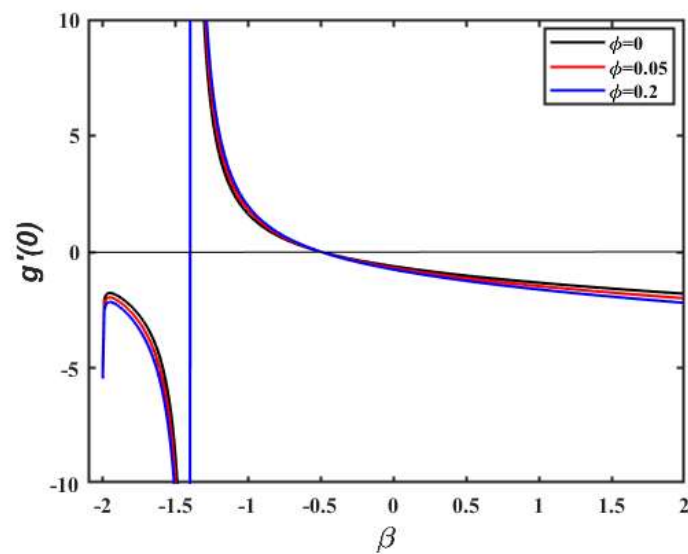


Figure 7. Variation of $g'(0)$ against β .

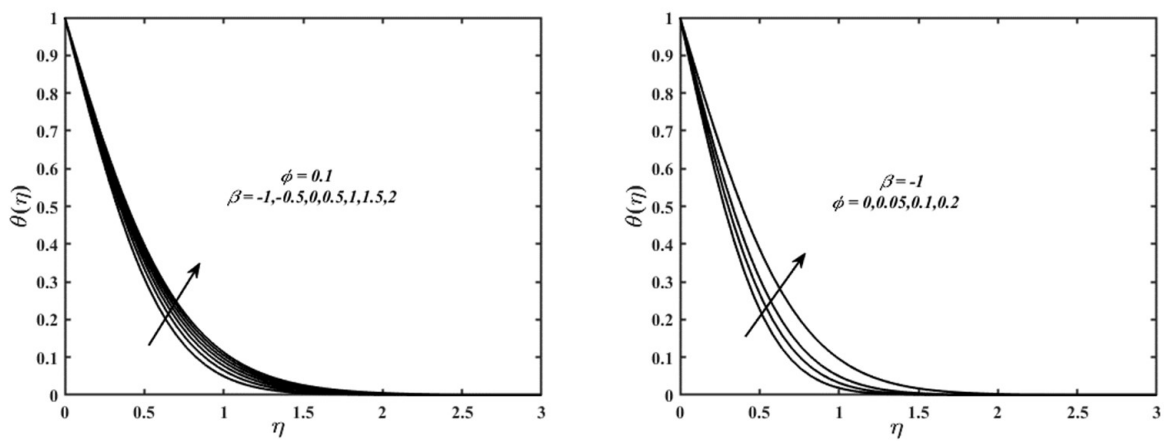


Figure 8. Variation of temperature profile $\theta(\eta)$ as a function of β and ϕ . The arrow shows course of cumulative ϕ .

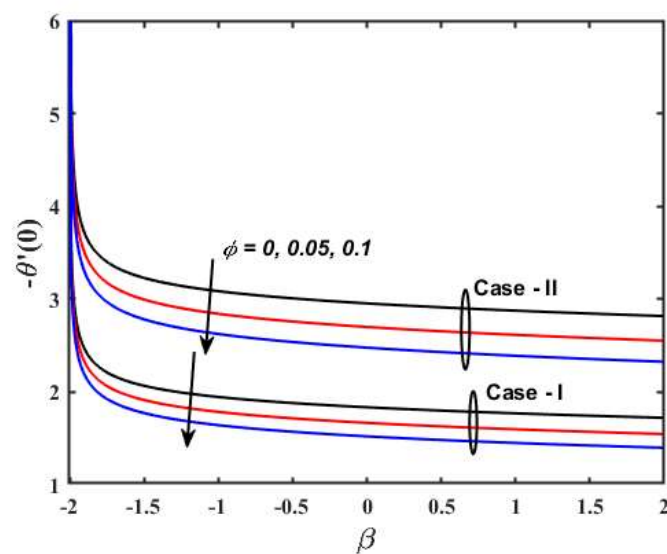


Figure 9. Variation of $-\theta'(0)$ against β for different values of ϕ .

6. Concluding Remarks

The main aim was to find exact solutions of nanofluid flow through the nonlinear stretched surface for streamwise, uniform and through transverse wall-shearing flows. In this present work, it is explored whether the boundary layer thickness is controlled by nanoparticle volume fraction. In addition, it is worth mentioning here that the nanoparticle volume fraction reduction in the heat flux at the surface has a higher value in case-II and a lower value in case-I. Furthermore, remarkably this one is determined for the longitudinal parameter of wall shear stress is greater than or of the same degree, in association with the transverse wall situation in the presence of nanoparticle volume fraction. However, these consequences in two parametric schemes of the equation are reliant on ϕ and σ . However, individual parameters of the solution are impartially reliant on nanoparticle

volume fraction ϕ through the selection of $\sigma = \begin{cases} \frac{(m+1)}{2} \\ nm, \text{ for } n \text{ to be an integer} \end{cases}$.

The present work will be similarly extended by assuming an exponential stretching sheet rather than the assumed nonlinear stretching sheet. In addition, we can study the streamwise flow with the cross flow of different types of non-Newtonian fluids on a nonlinear/exponential stretching sheet.

Author Contributions: Conceptualization, A.U.K.; Methodology, S.; Software, F.Z.D.; Investigation, A.U.K.; Resources, F.Z.D. and S.; Writing – original draft, A.U.K. and S.; Writing—review & editing, S.S.; Supervision, F.Z.D.; Project administration, S.; Funding acquisition, S.S. All authors have read and agreed to the published version of the manuscript.

Funding: Researchers supporting project number (RSPD2023R535), King Saud University, Riyadh, Saudi Arabia.

Data Availability Statement: Not applicable.

Acknowledgments: The authors extend their appreciation to the Deanship of Scientific Research at King Khalid University for funding this work through research groups program under Grant No. RGP.1/276/43.

Conflicts of Interest: The authors declare no conflict of interest.

Nomenclature

Symbols	Meaning and Dimension	Dimensionless Symbols
x, y, z	Cartesian coordinates [L]	η
u, v, w	Velocity components [L T ⁻¹]	f, g
T	Temperature profile [K]	θ
C_p	Specific heat capacity [ML ² K ⁻¹ T ⁻²]	
Greek symbols		
μ	Dynamic viscosity [M L ⁻¹ T ⁻¹]	–
ν	Kinematic viscosity [L ⁻² T ⁻¹]	–
ρ	Density [M L ⁻³]	–
β	Nonlinear stretching parameter	–
k	Thermal conductivity [Wm ⁻¹ K ⁻¹]	–
ϕ	Nanoparticle volume fraction	–
α	Thermal diffusivity [L ⁻² T ⁻¹]	
Subscripts		
f	Fluid	–
s	Solid fraction	–
nf	Nanofluid	–

References

1. Blasius, H. *Grenzschichten in Flüssigkeiten mit Kleiner Reibung*; Druck von BG Teubner: Berlin, Germany, 1907.
2. Prandtl, L. Über Flüssigkeitsbewegung bei sehr kleiner Reibung. In *Verhandl. III, Internat. Math.-Kong*; Teubner: Heidelberg, Germany, 1904; pp. 484–491.
3. Prandtl, L. On Boundary Layers in Three-Dimensional Flow. *Rep. Trans.* **1946**, *64*, 1–12.
4. Vvedenskaya, N.D. Three-dimensional laminar boundary layer on a blunt body. *Fluid Dyn.* **1966**, *1*, 25–28. [[CrossRef](#)]
5. Hayat, T.; Muhammad, T.; Shehzad, S.A.; Alsaedi, A. A Mathematical Study for Three-Dimensional Boundary Layer Flow of Jeffrey Nanofluid. *Z. Nat.* **2015**, *70*, 225–233. [[CrossRef](#)]
6. Kumar, K.G.; Haq, R.U.; Rudraswamy, N.; Gireesha, B. Effects of mass transfer on MHD three dimensional flow of a Prandtl liquid over a flat plate in the presence of chemical reaction. *Results Phys.* **2017**, *7*, 3465–3471. [[CrossRef](#)]
7. Hayat, T.; Aziz, A.; Muhammad, T.; Alsaedi, A. Three-dimensional flow of Prandtl fluid with Cattaneo-Christov double diffusion. *Results Phys.* **2018**, *9*, 290–296. [[CrossRef](#)]
8. Takhar, H.S.; Chamkha, A.J.; Nath, G. Unsteady three-dimensional MHD-boundary-layer flow due to the impulsive motion of a stretching surface. *Acta Mech.* **2001**, *146*, 59–71. [[CrossRef](#)]
9. Affes, H.; Xiao, Z.; Conlisk, A.T. The boundary-layer flow due to a vortex approaching a cylinder. *J. Fluid Mech.* **1994**, *275*, 33–57. [[CrossRef](#)]
10. Ahmad, K.; Nazar, R.; Ishak, A.; Pop, I. Unsteady three-dimensional boundary layer flow due to a stretching surface in a micropolar fluid. *Int. J. Numer. Methods Fluids* **2011**, *68*, 1561–1573. [[CrossRef](#)]
11. Weidman, P.D. New solutions for laminar boundary layers with cross flow. *Z. Angew. Math. Und Phys. ZAMP* **1997**, *48*, 341–356. [[CrossRef](#)]
12. Chu, Y.-M.; Khan, U.; Zaib, A.; Shah, S.H.A.M.; Marin, M. Numerical and Computer Simulations of Cross-Flow in the Streamwise Direction through a Moving Surface Comprising the Significant Impacts of Viscous Dissipation and Magnetic Fields: Stability Analysis and Dual Solutions. *Math. Probl. Eng.* **2020**, *2020*, 8542396. [[CrossRef](#)]
13. Dauenhauer, E.C.; Majdalani, J. Exact self-similarity solution of the Navier–Stokes equations for a porous channel with orthogonally moving walls. *Phys. Fluids* **2003**, *15*, 1485–1495. [[CrossRef](#)]
14. Roşca, N.C.; Roşca, A.V.; Jafarimoghaddam, A.; Pop, I. Cross flow and heat transfer past a permeable stretching/shrinking sheet in a hybrid nanofluid. *Int. J. Numer. Methods Heat Fluid Flow* **2020**, *31*, 1295–1319. [[CrossRef](#)]
15. Weidman, P. Further solutions for laminar boundary layers with cross flows driven by boundary motion. *Acta Mech.* **2017**, *228*, 1979–1991. [[CrossRef](#)]
16. Rashidi, S.; Dehghan, M.; Ellahi, R.; Riaz, M.; Jamal-Abad, M. Study of stream wise transverse magnetic fluid flow with heat transfer around an obstacle embedded in a porous medium. *J. Magn. Magn. Mater.* **2015**, *378*, 128–137. [[CrossRef](#)]
17. Bhattacharyya, K.; Pop, I. Heat transfer for boundary layers with cross flow. *Chin. Phys. B* **2014**, *23*, 024701. [[CrossRef](#)]
18. Zhong, L.; Zhou, C.; Chen, S. Effects of approaching main flow boundary layer on flow and cooling performance of an inclined jet in cross flow. *Int. J. Heat Mass Transf.* **2016**, *103*, 572–581. [[CrossRef](#)]
19. Yufeng, H.; Shaoxian, M.; Caihong, S. Numerical study on cross-flow transition in three-dimensional hypersonic boundary layers. *Acta Aerodyn. Sin.* **2019**, *37*, 522–529.
20. Crane, L.J. Flow past a stretching plate. *Z. Angew. Math. Und Phys. ZAMP* **1970**, *21*, 645–647. [[CrossRef](#)]
21. Khan, W.; Pop, I. Boundary-layer flow of a nanofluid past a stretching sheet. *Int. J. Heat Mass Transf.* **2010**, *53*, 2477–2483. [[CrossRef](#)]
22. Makinde, O.; Aziz, A. Boundary layer flow of a nanofluid past a stretching sheet with a convective boundary condition. *Int. J. Therm. Sci.* **2011**, *50*, 1326–1332. [[CrossRef](#)]
23. Mukhopadhyay, S. Slip effects on MHD boundary layer flow over an exponentially stretching sheet with suction/blowing and thermal radiation. *Ain Shams Eng. J.* **2013**, *4*, 485–491. [[CrossRef](#)]
24. Mahmud, K.; Rana, S.; Al-Zubaidi, A.; Mehmood, R.; Saleem, S. Interaction of Lorentz force with cross swimming microbes in couple stress nano fluid past a porous Riga plate. *Int. Commun. Heat Mass Transf.* **2022**, *138*, 106347. [[CrossRef](#)]
25. Tabassum, R.; Al-Zubaidi, A.; Rana, S.; Mehmood, R.; Saleem, S. Slanting transport of hybrid (MWCNTs-SWCNTs/H₂O) nanofluid upon a Riga plate with temperature dependent viscosity and thermal jump condition. *Int. Commun. Heat Mass Transf.* **2022**, *135*, 106165. [[CrossRef](#)]
26. Mahmud, K.; Mehmood, R.; Rana, S.; Al-Zubaidi, A. Flow of magnetic shear thinning nano fluid under zero mass flux and hall current. *J. Mol. Liq.* **2022**, *352*, 118732. [[CrossRef](#)]
27. Rana, S.; Mehmood, R.; Muhammad, T. On homogeneous-heterogeneous reactions in oblique stagnation-point flow of Jeffrey fluid involving Cattaneo-Christov heat flux. *Therm. Sci.* **2021**, *25*, 165–172. [[CrossRef](#)]
28. Rana, S.; Mehmood, R.; Bhatti, M.M.; Hassan, M. Swimming of motile gyrotactic microorganisms and suspension of nanoparticles in a rheological Jeffery fluid with Newtonian heating along elastic surface. *J. Cent. South Univ.* **2021**, *28*, 3279–3296. [[CrossRef](#)]
29. Mehmood, R.; Khan, S.; Maraj, E.N.; Ijaz, S.; Rana, S. Heat transport mechanism via ion-slip and Hall current in viscoplastic flow along a porous elastic sheet. *Proc. Inst. Mech. Eng. Part E J. Process. Mech. Eng.* **2021**, *236*, 907–914. [[CrossRef](#)]
30. Mehmood, R.; Rana, S.; Maraj, E.N. Transverse Transport of Polymeric Nanofluid under Pure Internal Heating: Keller Box Algorithm. *Commun. Theor. Phys.* **2018**, *70*, 106. [[CrossRef](#)]
31. Navier, C. Mémoire sur les lois du mouvement des fluides. *Mémoires L'académie R. Sci. L'institut Fr.* **1823**, *6*, 389–440.

32. Martin, M.J.; Boyd, I.D. Blasius boundary layer solution with slip flow conditions. *AIP Conf. Proc.* **2001**, *585*, 518–523.
33. Rao, I.J.; Rajagopal, K.R. The effect of the slip boundary condition on the flow of fluids in a channel. *Acta Mech.* **1999**, *135*, 113–126. [[CrossRef](#)]
34. Ellahi, R. Effects of the slip boundary condition on non-Newtonian flows in a channel. *Commun. Nonlinear Sci. Numer. Simul.* **2009**, *14*, 1377–1384. [[CrossRef](#)]
35. Hayat, T.; Khan, M.; Ayub, M. On non-linear flows with slip boundary condition. *Z. Angew. Math. Und Phys. ZAMP* **2005**, *56*, 1012–1029. [[CrossRef](#)]
36. Nandeppanavar, M.M.; Vajravelu, K.; Abel, M.S.; Siddalingappa, M. Second order slip flow and heat transfer over a stretching sheet with non-linear Navier boundary condition. *Int. J. Therm. Sci.* **2012**, *58*, 143–150. [[CrossRef](#)]
37. Oyelakin, I.S.; Mondal, S.; Sibanda, P. Unsteady Casson nanofluid flow over a stretching sheet with thermal radiation, convective and slip boundary conditions. *Alex. Eng. J.* **2016**, *55*, 1025–1035. [[CrossRef](#)]
38. Ariel, P.D.; Hayat, T.; Asghar, S. The flow of an elastico-viscous fluid past a stretching sheet with partial slip. *Acta Mech.* **2006**, *187*, 29–35. [[CrossRef](#)]
39. Noghrehabadi, A.; Saffarian, M.R.; Pourrajab, R.; Ghalambaz, M. Entropy analysis for nanofluid flow over a stretching sheet in the presence of heat generation/absorption and partial slip. *J. Mech. Sci. Technol.* **2013**, *27*, 927–937. [[CrossRef](#)]
40. Gupta, P.; Gupta, A. Heat and mass transfer on a stretching sheet with suction or blowing. *Can. J. Chem. Eng.* **1977**, *55*, 744–746. [[CrossRef](#)]
41. Vajravelu, K. Viscous flow over a nonlinearly stretching sheet. *Appl. Math. Comput.* **2001**, *124*, 281–288. [[CrossRef](#)]
42. Cortell, R. Viscous flow and heat transfer over a nonlinearly stretching sheet. *Appl. Math. Comput.* **2007**, *184*, 864–873. [[CrossRef](#)]
43. Das, K. Nanofluid flow over a non-linear permeable stretching sheet with partial slip. *J. Egypt. Math. Soc.* **2015**, *23*, 451–456. [[CrossRef](#)]
44. Seth, G.; Mishra, M. Analysis of transient flow of MHD nanofluid past a non-linear stretching sheet considering Navier’s slip boundary condition. *Adv. Powder Technol.* **2017**, *28*, 375–384. [[CrossRef](#)]
45. Mukhopadhyay, S. Analysis of boundary layer flow over a porous nonlinearly stretching sheet with partial slip at the boundary. *Alex. Eng. J.* **2013**, *52*, 563–569. [[CrossRef](#)]
46. Choi, S.; Eastman, J.A. *Enhancing Thermal Conductivity of Fluids with Nanoparticles*; No. ANL/MSD/CP-84938; CONF-951135-29; Argonne National Lab.(ANL): Argonne, IL, USA, 1995.
47. Kang, H.U.; Kim, S.H.; Oh, J.M. Estimation of Thermal Conductivity of Nanofluid Using Experimental Effective Particle Volume. *Exp. Heat Transf.* **2006**, *19*, 181–191. [[CrossRef](#)]
48. Khan, A.U.; Saleem, S.; Nadeem, S.; Alderremy, A. Analysis of unsteady non-axisymmetric Homann stagnation point flow of nanofluid and possible existence of multiple solutions. *Phys. A Stat. Mech. Its Appl.* **2019**, *554*, 123920. [[CrossRef](#)]
49. Khan, A.; Hussain, S.; Nadeem, S. Existence and stability of heat and fluid flow in the presence of nanoparticles along a curved surface by mean of dual nature solution. *Appl. Math. Comput.* **2019**, *353*, 66–81. [[CrossRef](#)]
50. Duraihem, F.Z.; Akbar, N.S.; Saleem, S. Mixed convective eyring-powell ferro magnetic nanofluid flow suspension towards a stretching surface with buoyancy effects through numerical analysis. *Front. Mater.* **2023**, *10*, 1109755. [[CrossRef](#)]
51. Nadeem, S.; Khan, M.R.; Khan, A.U. MHD oblique stagnation point flow of nanofluid over an oscillatory stretching/shrinking sheet: Existence of dual solutions. *Phys. Scr.* **2019**, *94*, 075204. [[CrossRef](#)]
52. Ali, A.; Khan, H.S.; Saleem, S.; Hussain, M. EMHD nanofluid flow with radiation and variable heat flux effects along a Slandering stretching sheet. *Nanomaterials* **2022**, *12*, 3872. [[CrossRef](#)]
53. Hayat, T.; Nadeem, S.; Khan, A.U. Rotating flow of Ag-CuO/H₂O hybrid nanofluid with radiation and partial slip boundary effects. *Eur. Phys. J. E* **2018**, *41*, 1–9. [[CrossRef](#)]
54. Sivaraj, R.; Animasaun, I.L.; Olabiyi, A.S.; Saleem, S.; Sandeep, N. Gyrotactic microorganisms and thermoelectric effects on the dynamics of 29nmCuO-water nanofluid over an upper horizontal surface of paraboloid of revolution. *Multidiscip. Model. Mater. Struct.* **2018**, *14*, 695–6721. [[CrossRef](#)]
55. Amanulla, C.H.; Saleem, S.; Wakif, A.; AlQarni, M.M. MHD Prandtl fluid flow past an isothermal sphere with slip effects: Non-Darcy porous medium. *Case Stud. Therm. Eng.* **2019**, *14*, 100447. [[CrossRef](#)]
56. Nawaz, M.; Nazir, U.; Saleem, S.; Alharbi, S.O. An enhancement of thermal performance of ethylene glycol by nano and hybrid nanoparticles. *Phys. A Stat. Mech. Its Appl.* **2020**, *551*, 124527. [[CrossRef](#)]
57. Weidman, P. Similarity solutions for power-law and exponentially stretching plate motion with cross flow. *Int. J. Non-Linear Mech.* **2017**, *89*, 127–131. [[CrossRef](#)]
58. Banks, W. Similarity solutions of the boundary-layer equations for a stretching wall. *J. Mécanique Théorique Appliquée* **1983**, *2*, 375–392.
59. Dinarvand, S.; Hosseini, R.; Damangir, E.; Pop, I. Series solutions for steady three-dimensional stagnation point flow of a nanofluid past a circular cylinder with sinusoidal radius variation. *Meccanica* **2012**, *48*, 643–652. [[CrossRef](#)]

Disclaimer/Publisher’s Note: The statements, opinions and data contained in all publications are solely those of the individual author(s) and contributor(s) and not of MDPI and/or the editor(s). MDPI and/or the editor(s) disclaim responsibility for any injury to people or property resulting from any ideas, methods, instructions or products referred to in the content.